NRL Report 7596

Sustained-Load Cracking of Titanium

A Survey of 6Al-4V Alloys

G. R. YODER, C. A. GRIFFIS, AND
T. W. CROOKER

Strength of Metals Branch
Metallurgy Division

August 24, 1973

NAVAL RESEARCH LABORATORY
Washington, D.C.

Approved for public release; distribution unlimited.

Security Classification

DOCUMENT CONTROL DATA - R & D

(Security classification of title, body of abstract and indexing annotation must be entered when the overall report is classified)

1. ORIGINATING ACTIVITY *(Corporate author)* Naval Research Laboratory Washington, D.C. 20375	2a. REPORT SECURITY CLASSIFICATION Unclassified 2b. GROUP

3. REPORT TITLE

SUSTAINED-LOAD CRACKING OF TITANIUM: A SURVEY OF 6A1-4V ALLOYS

4. DESCRIPTIVE NOTES *(Type of report and inclusive dates)*

Final report on one phase of a continuing NRL Problem.

5. AUTHOR(S) *(First name, middle initial, last name)*

G. R. Yoder, C. A. Griffis, and T. W. Crooker

6. REPORT DATE August 24, 1973	7a. TOTAL NO. OF PAGES 24	7b. NO. OF REFS 23
8a. CONTRACT OR GRANT NO. NRL Problems M01-25 and M01-28 b. PROJECT NO. Projects RR 022-01-46-5432 and c. WR 022-10-01 d.	9a. ORIGINATOR'S REPORT NUMBER(S) NRL Report 7596 9b. OTHER REPORT NO(S) *(Any other numbers that may be assigned this report)*	

10. DISTRIBUTION STATEMENT

Approved for public release; distribution unlimited.

11. SUPPLEMENTARY NOTES	12. SPONSORING MILITARY ACTIVITY Department of the Navy Office of Naval Research Arlington, Virginia 22217

13. ABSTRACT

This survey reveals that degradation in load-carrying capacity owing to sustained-load cracking (SLC) is widespread and serious in alloys of the Ti-6A1-4V family. Each of eight different 1-in. (2.5-cm) thick plates tested in air at room temperature exhibited the effect, with degradations ranging up to 35%. The amount of degradation does not seem to correlate with differences in hydrogen content, processing variables, or strength and toughness levels; however, the susceptibility to SLC is orientation dependent. Invalidity of several of the rising-load fracture toughness values, with respect to plane-strain criteria, makes quantitative comparison of degradations uncertain. However, the threshold stress-intensity factor below which SLC failures will not occur, K_{It}, clearly represents a more conservative fracture-safe design parameter than the plane-strain fracture toughness K_{Ic}, which cannot account for insidious time-delayed failures owing to SLC.

DD FORM 1 NOV 65 1473 (PAGE 1)

S/N 0101-807-6801

Security Classification

Security Classification

14. KEY WORDS	LINK A ROLE	LINK A WT	LINK B ROLE	LINK B WT	LINK C ROLE	LINK C WT
Titanium alloys						
Sustained-load cracking						
Subcritical crack growth						
Fracture toughness						
Fracture mechanics						
Fracture						

DD FORM 1 NOV 65 1473 (BACK)
(PAGE 2)

Security Classification

CONTENTS

Abstract ii
Problem Status ii
Authorization ii
Nomenclature iii

INTRODUCTION 1

PROCEDURE 1

RESULTS 4

DISCUSSION 11

SUMMARY 16

ACKNOWLEDGMENTS 17

REFERENCES 17

ABSTRACT

This survey reveals that degradation in load-carrying capacity owing to sustained-load cracking (SLC) is widespread and serious in alloys of the Ti-6Al-4V family. Each of eight different 1-in. (2.5-cm) thick plates tested in air at room temperature exhibited the effect, with degradations ranging up to 35%. The amount of degradation does not seem to correlate with differences in hydrogen content, processing variables, or strength and toughness levels; however, the susceptibility to SLC is orientation dependent. Invalidity of several of the rising-load fracture toughness values, with respect to plane-strain criteria, makes quantitative comparison of degradations uncertain. However, the threshold stress-intensity factor below which SLC failures will not occur, K_{It}, clearly represents a more conservative fracture-safe design parameter than the plane-strain fracture toughness K_{Ic}, which cannot account for insidious time-delayed failures owing to SLC.

PROBLEM STATUS

This report completes one phase of the problem; work on other aspects of the problem is continuing.

AUTHORIZATION

NRL Problems M01-25 and M01-28
Projects RR 022-01-46-5432 and WR 022-01-01

Manuscript submitted April 18, 1973.

NOMENCLATURE

A	lumped material constant
a	crack depth
B	plate thickness
C	constant (4.12 for cantilever loading, 3.80 for three-point bending)
c	concentration of hydrogen at the crack tip
c_0	concentration of hydrogen in the bulk
$2c$	length (major axis of surface crack)
D	specimen height; diffusivity
D_0	diffusion constant
$\dot{K}$	time derivative of stress-intensity factor
k	Boltzmann's constant
K_{Ic}	plane-strain fracture toughness
K_{Ii}	stress-intensity factor, based on initial crack length
K_{Ir}	stress-intensity factor, fracture resistance from rising-load test
K_{It}	threshold stress-intensity factor below which SLC failures will not occur
K_Q	stress-intensity factor, defined by ASTM-E399 5% secant offset method, from load displacement record
L	constant with dimension of length
M	applied bending moment
$\dot{P}$	time derivative of load
P_{max}	maximum load
P_Q	load defined by ASTM-E399 5% secant offset method, from load displacement record

PTC	part-through surface-cracked tension specimen
ppm	parts per million by weight
Q	flaw shape factor
r	radial polar coordinate
S	short transverse direction (thickness)
SEN	single-edge-notch bend specimen
SLC	sustained-load cracking
T	absolute temperature; long transverse direction
t_f	time to failure
$\bar{v}$	drift velocity
V	interaction energy between diffusing hydrogen and the crack-tip stress field
α	1 - a/D
Δ	SLC degradation in load-carrying capacity, in percent
θ	angular polar coordinate
σ	gross section stress
σ_{ys}	0.2% offset yield strength
τ	incubation time
∇	gradient

SUSTAINED-LOAD CRACKING OF TITANIUM: A SURVEY OF 6A1-4V ALLOYS

INTRODUCTION

While titanium alloys may be attractive for naval structural applications on the basis of high strength-to-density ratio, among other features, many exhibit potentially catastrophic crack (or flaw) extension while under static loads. Although such crack growth is usually attributable to stress-corrosion cracking, where aggressive environments are involved, it has also been reported for inert environments. In the latter case, crack growth has been referred to as sustained-load cracking (SLC), and has in several cases been attributed to the presence of interstitial hydrogen. The present effort to investigate SLC was motivated by the implications of this form of cracking with respect to structural life and proof testing. Results from the initial phase of this work, concerned primarily with determination of the SLC effect, are contained herein together with preliminary ramifications as to mechanism. Alloys examined, nominally from the 6A1-4V system, include both commercially and specially processed plates of widely divergent processing histories and interstitial contents.

The SLC phenomenon can be described with fracture mechanics parameters in the same manner that crack extension under static loading in an aggressive environment has been characterized for stress-corrosion cracking (1-3). Thus, if a material susceptible to SLC is loaded to initial stress-intensity K_{Ii} levels above a threshold level K_{It}, it will fail after a delay time t_f which decreases with increasing K_{Ii}. Delay times associated with this form of subcritical crack growth sometimes amount to several hours, and the threshold levels are as much as 35% less than the fracture resistance implied from standardized fracture toughness tests of only a few minutes' duration.

Awareness of SLC in titanium alloys dates back to the mid-1950's, when Burte *et al.* (4) demonstrated the time-delayed failure phenomenon with room-temperature stress-rupture tests of notched specimens in ambient air. The results of their work strongly implied that SLC behavior is due to hydrogen-assisted cracking, inasmuch as the phenomenon disappeared when the hydrogen content was reduced below a critical level known as the hydrogen tolerance. Later experiments by Sandoz (5) and Meyn (6), performed with fatigue-precracked specimens, suggested that the tolerance levels in titanium alloys based on the notched specimens were grossly overestimated, owing to the notch acuity effect demonstrated by Troiano (7), who found that the sharper the notch of the test specimen, the lower the apparent hydrogen content required for SLC of steels. Other reports of SLC in titanium alloys in ambient air have been made by Chu (8); Lane, Cavallaro, and Morton (9); and others (10).

PROCEDURE

Two specimen types were employed, the part-through surface cracked (PTC) tension specimen and the single-edge-notch (SEN) bend specimen, illustrated in Fig. 1. The latter

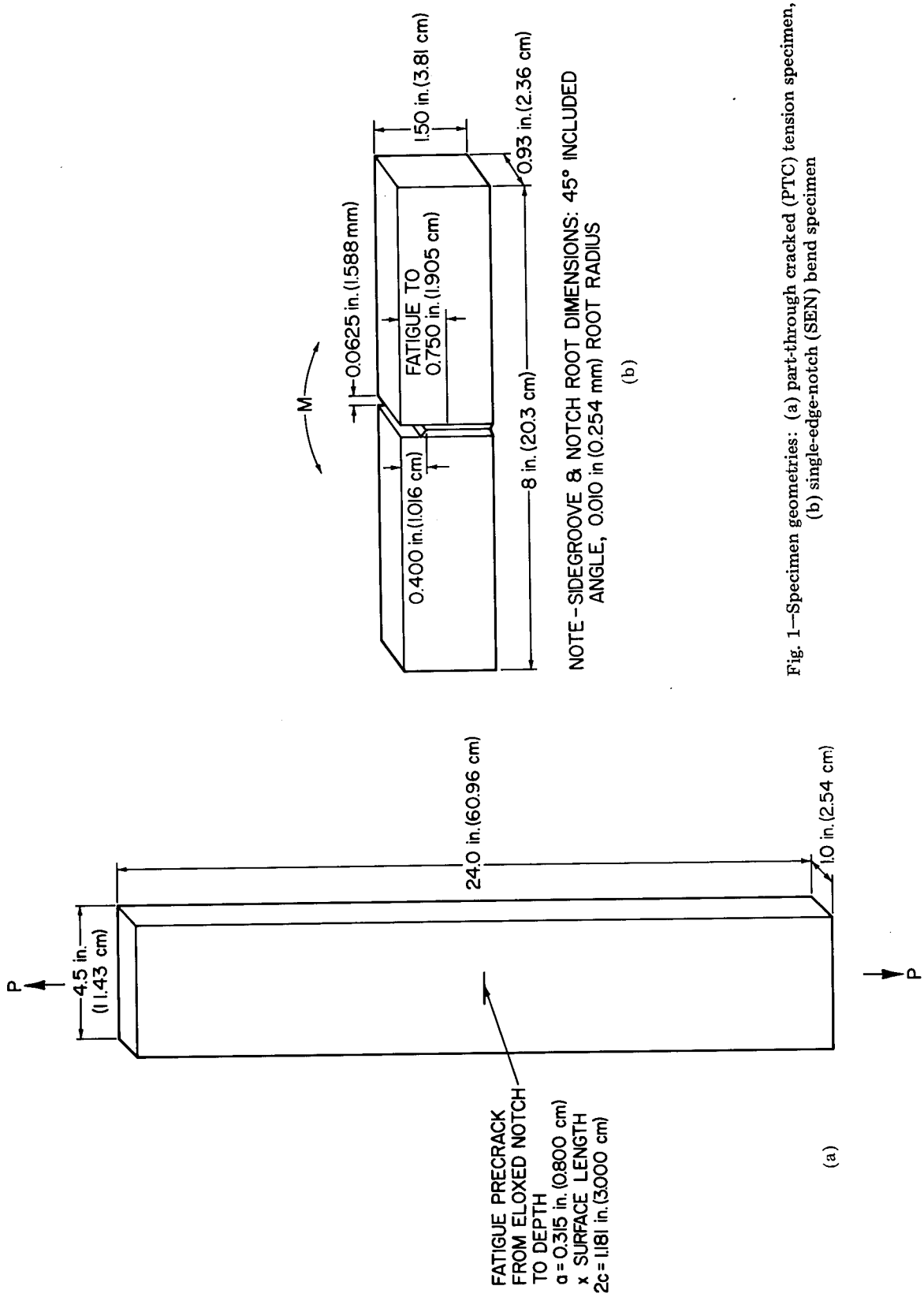

Fig. 1—Specimen geometries: (a) part-through cracked (PTC) tension specimen, (b) single-edge-notch (SEN) bend specimen

type was used for the rising-load three-point bend test. For the SEN bend specimens, the K_{Ii} were computed from

$$K_{Ii} = CM \frac{\sqrt{\frac{1}{\alpha^3} - \alpha^3}}{BD^{3/2}} \tag{1}$$

where

C = 4.12 for cantilever loading (11) and 3.80 for rising-load bend tests (12)

M = applied bending moment

B = specimen thickness

D = specimen height

α = 1 - a/D (a = initial crack length).

For the PTC tension specimens (13),

$$K_{Ii} = 1.1\,\sigma \sqrt{\pi \frac{a}{Q}} \tag{2}$$

where

σ = gross section stress

Q = flaw shape factor.

While all specimens were cut from 1-in. (2.5-cm) thick plate, different crack orientations were used for the two specimen types, viz. TS and TL (14) for the PTC and SEN specimens, respectively.

The SEN specimens were sidegrooved to a depth of 0.05B per side; thus while B (gross) = 0.93 in. (2.36 cm), B (net) = 0.84 in. (2.13 cm) was used for calculations with Eq. (1). Other SEN specimen dimensions were D = 1.50 in. (3.81 cm), a $\approx$ 0.750 in. (1.91 cm), with specimen length = 8 in. (20.3 cm). For three-point bend tests, a span of 6 in. (15.24 cm) between rollers was used, while a loading rate of $\dot{P} \approx$ 8.6 kips/min (38.2 kN/min) [$\dot{K} \approx$ 90 ksi$\sqrt{\text{in.}}$/min (100 MPa-m$^{1/2}$)] was employed. The SEN specimens were fatigue precracked and equipped with displacement gages spanning the crack notches, in accord with the ASTM specifications (15). Step loading was not employed in any of the dead-weight cantilever tests for reasons described by Chu (8); rather, the full load was applied in a single application. Furthermore, a few specimens which displayed crack arrest were retested only after refatiguing the blunted crack tip to a point safely beyond the bounds of the plastic zone.

The PTC specimens were 24 in. (60.96 cm) long, 1 in. (2.54 cm) thick, and either 4.0 in. (10.16 cm) wide for rising-load tests or 4.5 in. (11.43 cm) for sustained-load tensile tests. Unless otherwise indicated, these specimens were loaded at the rate $\dot{P}$ = 500 kips/s to either an appropriate level of sustained load or to failure in a rising-load test. These specimens were initially notched by electrical discharge machining, and then fatigue precracked to give "thumbnail" crack dimensions of approximately a/2c = 0.315 in. (0.800 cm)/1.181 in. (3.000 cm), where a is the crack length in the T direction of the plate and 2c is the major axis of the crack in the S direction. Fatigue precracking was accomplished by cycling the specimen between 0 and 225 kips (1000 kN) tension.

RESULTS

All plates tested exhibited SLC degradation in load-carrying capacity, more than 30% in some cases. In all instances, the greater portion of the apparent degradation occurred within a few hours of testing under sustained-load conditions. Results are summarized in Figs. 2-9 and Table 1. The table shows that materials examined ranged in (a) hydrogen contents from 35 to 80 parts per million by weight (ppm), (b) oxygen contents from 500 to 1600 ppm, (c) yield strengths (σ_{ys}) from 115 ksi (802 MPa) to 144 ksi (1005 MPa), (d) rolling temperatures from 1400°F (1033°K) to 1900°F (1311°K), and (e) forging temperature ranges from $\alpha + \beta$ to β. Each SLC curve in Figs. 2-9 is comprised of data points from both rising-load and sustained-load tests, the former of which are denoted by solid points, the latter with hollow points. From each curve the percentage of SLC degradation is measured as

$$\Delta = \left(1 - \frac{K_{It}}{K_{Ir}}\right) \times 100, \tag{3}$$

where K_{Ir} is the value of K_{Ii} from the rising-load test.

These degradations have been recorded in Table 1 together with other pertinent parameters which relate to the level of constraint represented by these tests. It is noted in the table that there are two possible values of K_{Ir} to choose from, viz. K_Q and K_{Imax}. The former is determined by the standard ASTM method from load-crack opening displacement traces (15), whereas the latter is calculated by using the maximum load value P_{max} from the same trace. As shown in the table, however, in most cases K_Q fails to meet the criteria for valid K_{Ic} numbers (14), viz.,

$$\frac{P_{max}}{P_Q} \leq 1.10 \tag{4}$$

$$2.5 \left(\frac{K_Q}{\sigma_{ys}}\right)^2 \leq B, a, D - a, \tag{5}$$

and is therefore a dubious parameter. Moreover, such an invalid K_Q number is not consistent with data from the sustained-load, cantilever bend tests. For example, in the case of alloy D4, $K_Q \approx 68$ ksi$\sqrt{\text{in.}}$ (75.6 MPa-m$^{1/2}$), while $K_{It} \approx 70$ ksi$\sqrt{\text{in.}}$ (77.9 MPa-m$^{1/2}$), and breaks appear at K_{Ii} = 73 and 77 ksi$\sqrt{\text{in.}}$ (81.2 and 85.7 MPa-m$^{1/2}$) in the sustained-load cantilever bend results, as displayed in Fig. 7. On the other hand, K_{Imax} = 80 ksi$\sqrt{\text{in.}}$ (90.0 MPa-m$^{1/2}$) is consistent with the cantilever bend data. To further

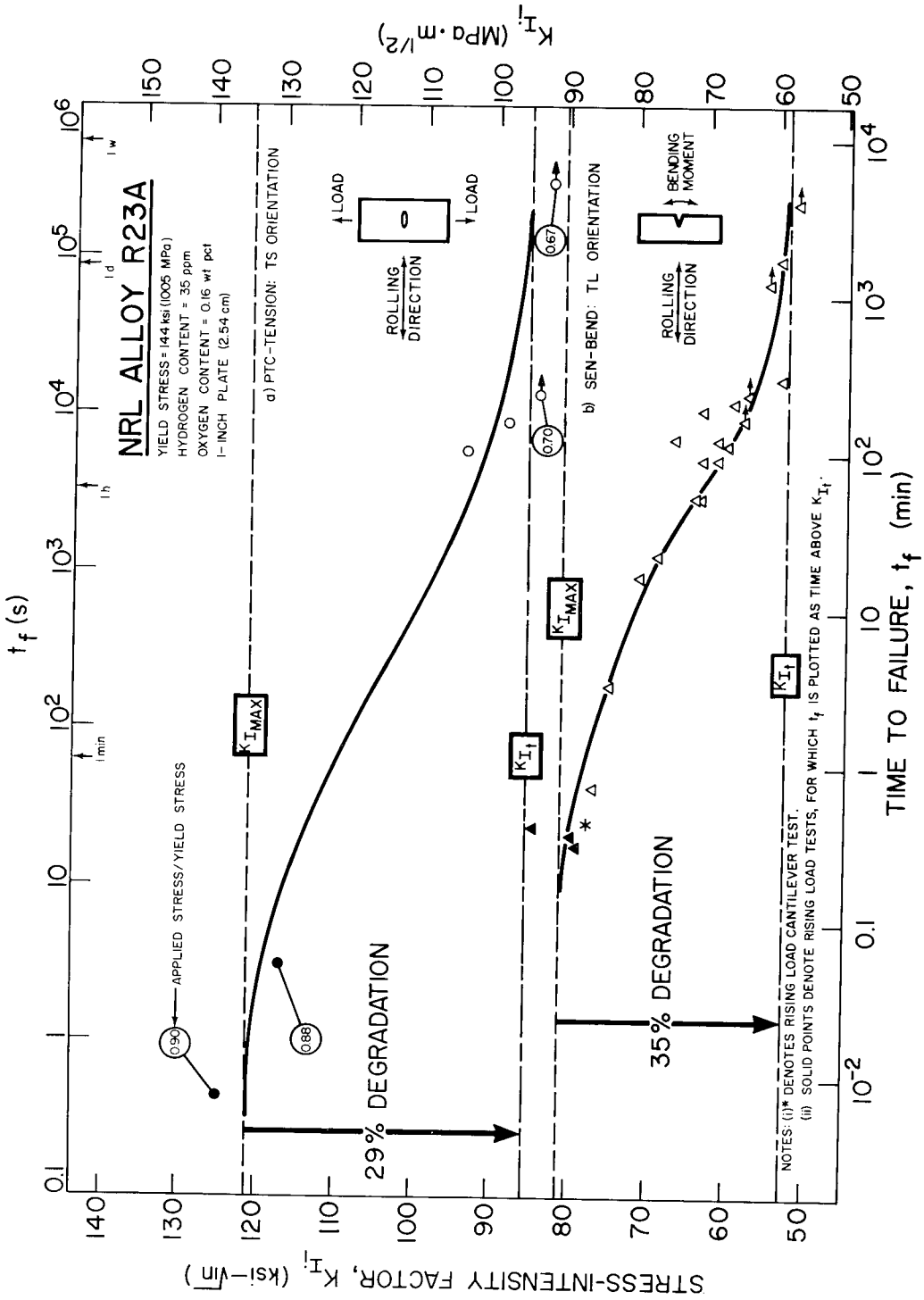

Fig. 2—Sustained load cracking in NRL alloy R23A in ambient, room-temperature air: (a) PTC tension specimens, (b) SEN bend specimens. Solid points represent rising-load tests; hollow points denote sustained-load tests.

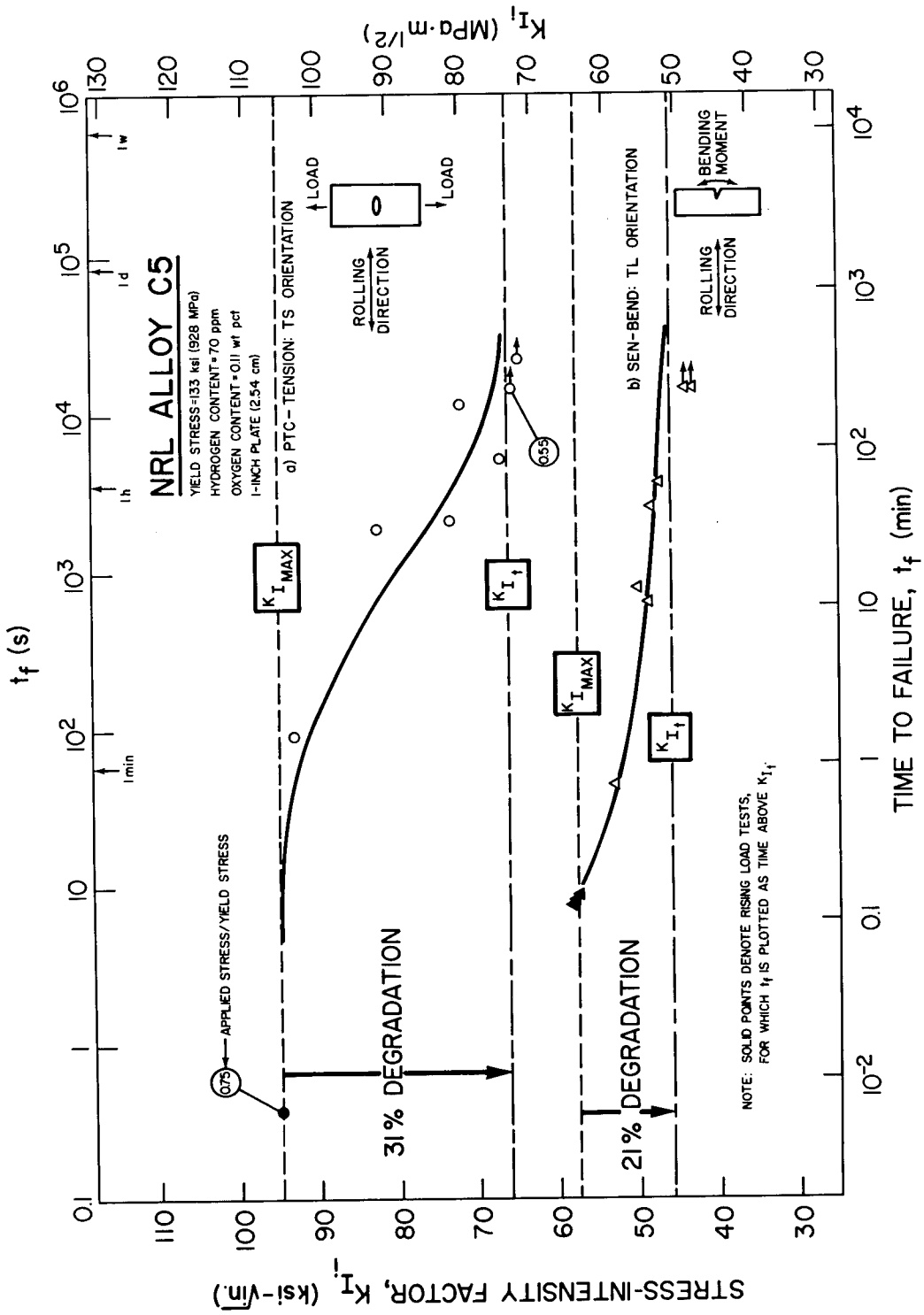

Fig. 3—Sustained-load cracking in NRL alloy C5 in ambient, room-temperature air: (a) PTC tension specimens, (b) SEN bend specimens. Solid points represent rising-load tests; hollow points denote sustained-load tests.

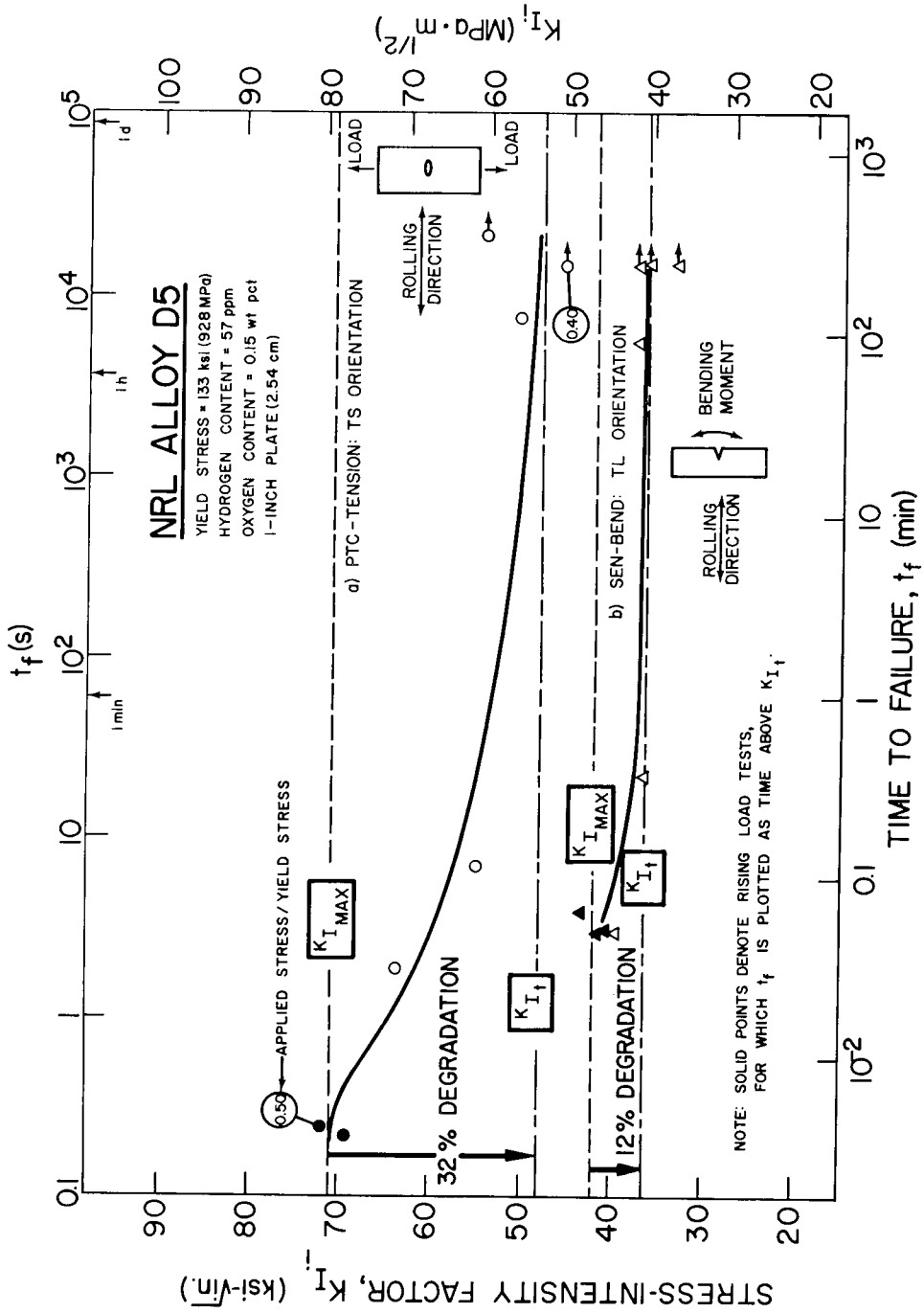

Fig. 4—Sustained-load cracking in NRL alloy D5 in ambient, room-temperature air: (a) PTC tension specimens, (b) SEN bend specimens. Solid points represent rising-load tests; hollow points denote sustained-load tests.

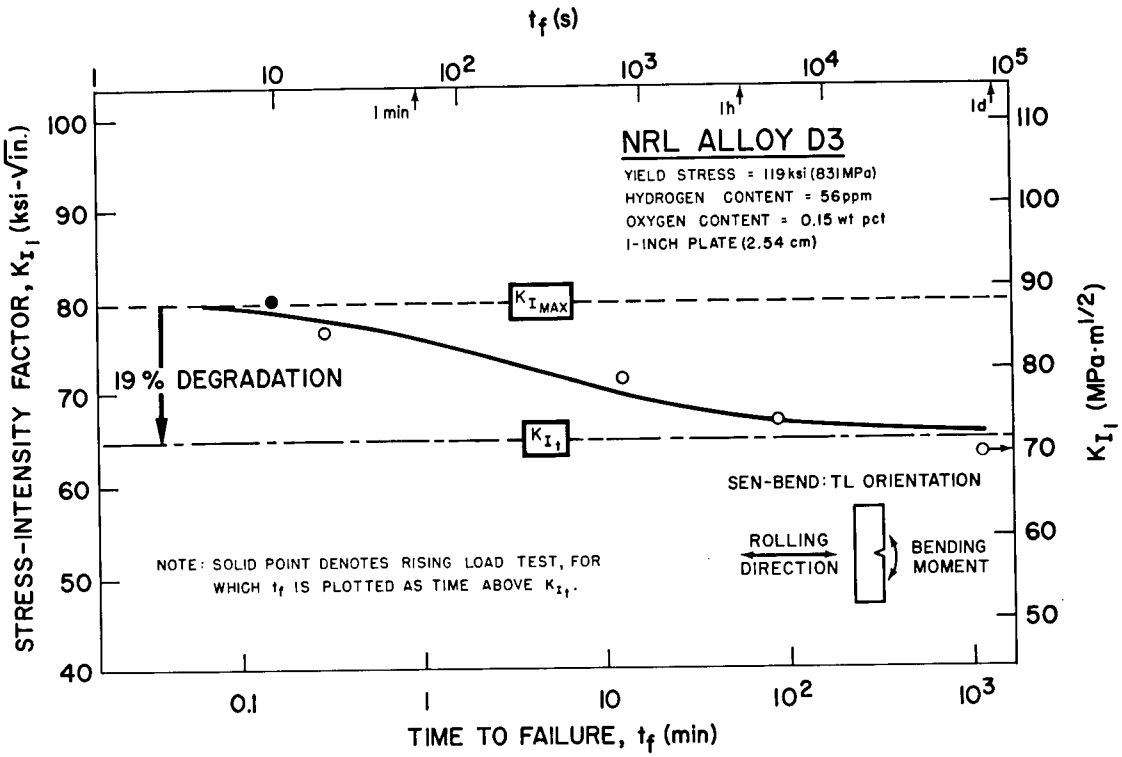

Fig. 5—Sustained-load cracking in NRL alloy D3 in ambient, room-temperature air; SEN bend specimens. Solid points represent rising-load tests; hollow points denote sustained-load tests.

corroborate an association between K_{Imax} from the rising-load three-point bend test and the cantilever bend data, a special test was devised using alloy R23A, wherein a rising-load cantilever bend test was performed by employing an Instron machine to drive downward the end of the cantilever bar. As illustrated in Fig. 2, this test indicated that K_{Imax} = 78 ksi$\sqrt{in.}$ (86.8 MPa-m$^{1/2}$), a value which compares favorably with numbers from the rising-load three-point bend tests, viz. K_{Imax} = 79, 80, 85 ksi$\sqrt{in.}$ (87.9, 89.0, 95.6 MPa-m$^{1/2}$). Therefore, $K_{Ir} = K_{Imax}$ is chosen for the computation of K_{It}/K_{Ir} in Eq. (3), as well as for the value of K_{Ii} displayed in Figs. 2-9 for rising-load test results.

Whereas every material tested exhibited degradation in load-carrying capacity owing to SLC, with Δ ranging from about 11 to 35%, for a given crack orientation Δ does not seem to correlate with other variables listed in Table 1, including hydrogen content.

A consideration of Figs. 2-4 (or Table 1) for comparison of results from plates tested in both the SEN and PTC specimen configurations, viz. alloys C5, R23A, and D5, shows that there are large discrepancies in the data for each material between threshold K_{It} values obtained from the two specimen types; similarly for the K_{Imax} values. For example, in the case of alloy C5, K_{It} = 66 and 46 ksi$\sqrt{in.}$ (73.4 and 51.2 MPa-m$^{1/2}$), while K_{Imax} = 95 and 58 ksi$\sqrt{in.}$ (105.7 and 64.5 MPa-m$^{1/2}$) for the PTC and SEN specimens, respectively; the consequent discrepancy in Δ is 31 vs 21%. These differences are probably attributable to anisotropy, since different crack orientations were used for the two specimen types. However, they may also in part be due to the invalid nature of the fracture toughness numbers, although for alloy D5, K_{It} values from both the PTC and SEN specimens satisfy the ASTM thickness requirement. The macrofractograph in

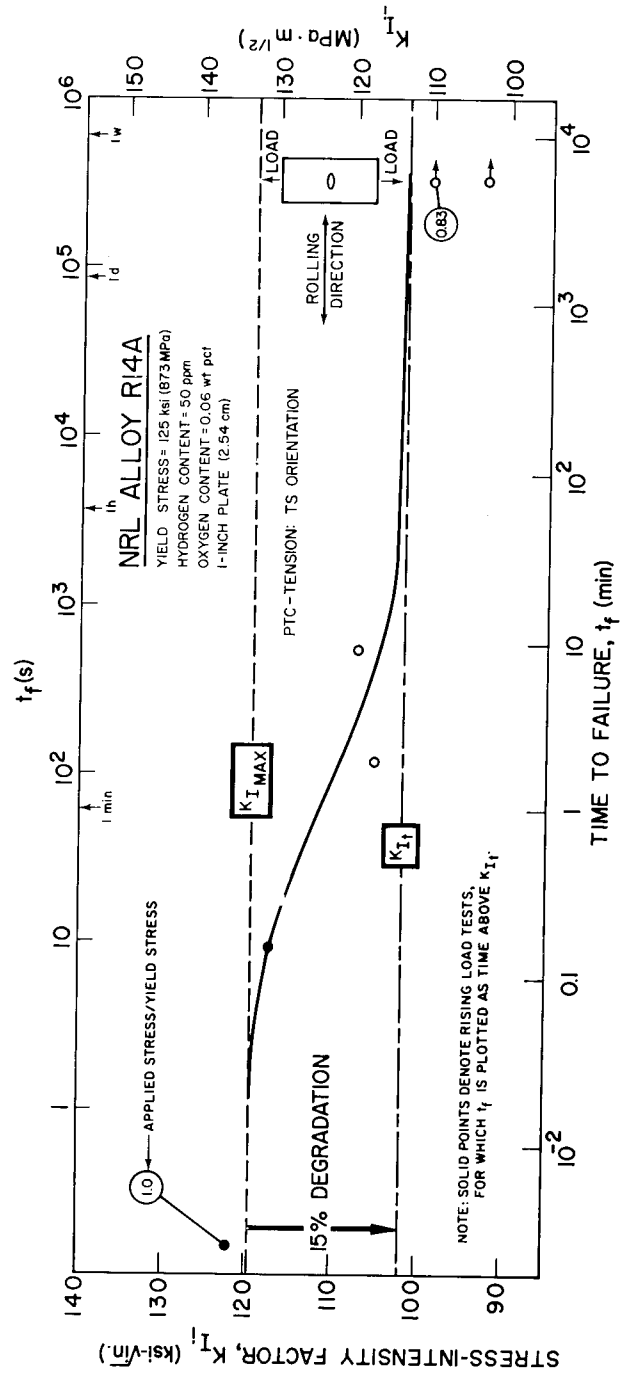

Fig. 6—Sustained-load cracking in NRL alloy R14A in ambient, room-temperature air; PTC tension specimens. Solid points represent rising-load tests; hollow points denote sustained-load tests.

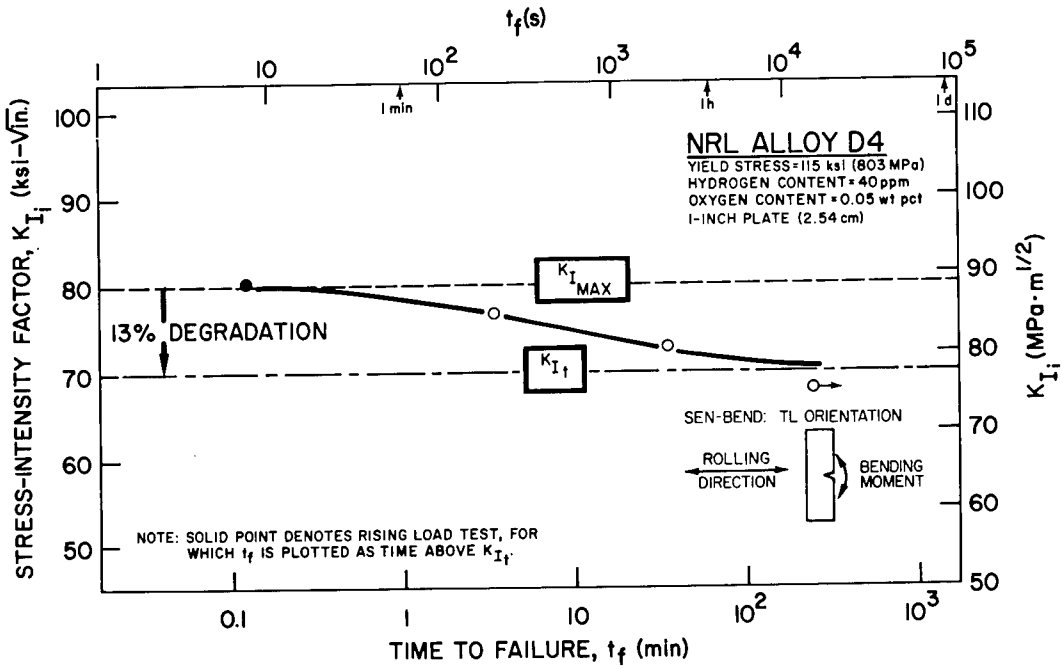

Fig. 7—Sustained-load cracking in NRL alloy D4 in ambient, room-temperature air, SEN bend specimens. Solid points represent rising-load tests; hollow points denote sustained-load tests.

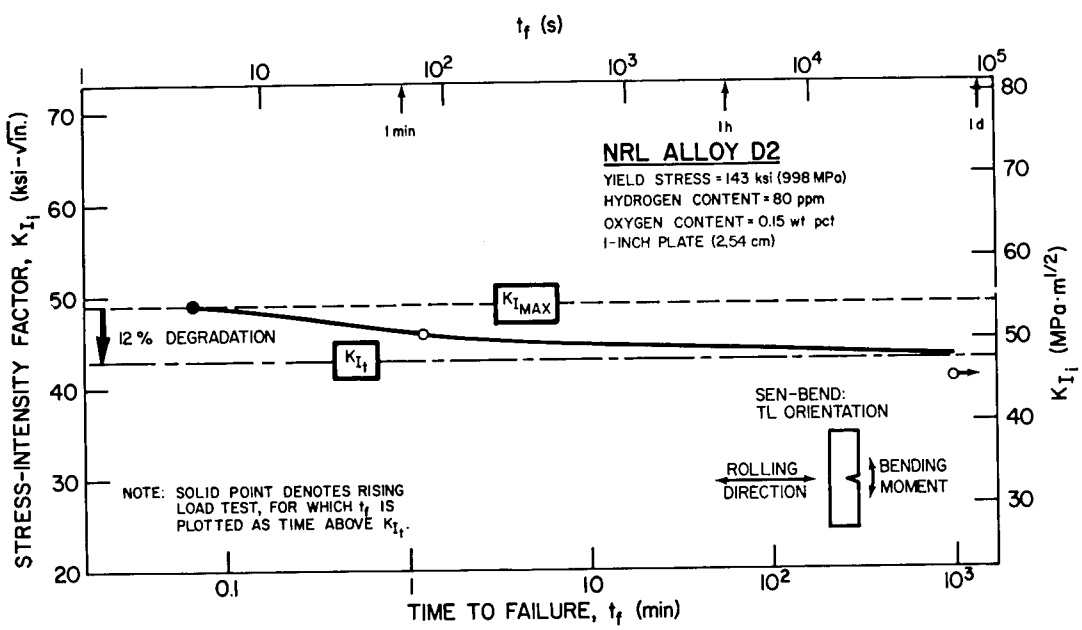

Fig. 8—Sustained-load cracking in NRL alloy D2 in ambient, room-temperature air; SEN bend specimens. Solid points represent rising-load tests; hollow points denote sustained-load tests.

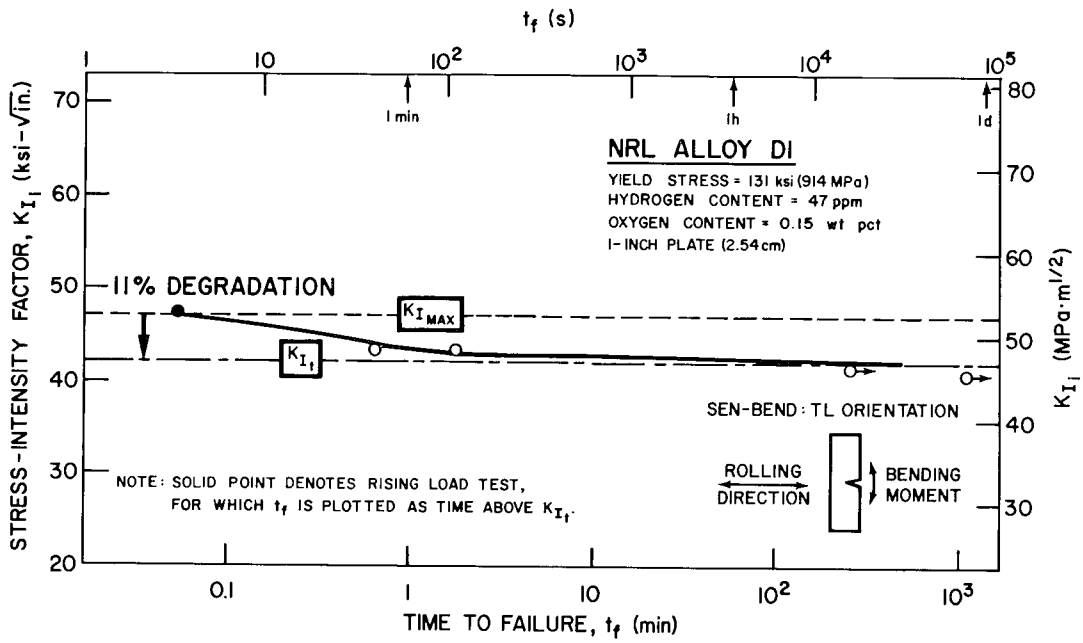

Fig. 9—Sustained-load cracking in NRL alloy D1 in ambient, room-temperature air; SEN bend specimens. Solid points represent rising-load tests; hollow points denote sustained-load tests.

Fig. 10 illustrates the anisotropy in SLC growth in a PTC specimen of alloy R23A. Growth in the region between dashed lines is less in the thickness direction (indicated by arrow) than in the transverse direction, although analysis of the maximum Mode I stress-intensity factor for a given applied load would predict greater growth in the thickness direction for an isotropic material. Scanning electron microscopy shows that SLC growth occurs in alloy R23A by both microvoid coalescence and cleavage. In the SEN bend specimen loaded to an initial K_{Ii} = 65 ksi$\sqrt{in.}$ (72.3 MPa-m$^{1/2}$), cleavage was found in decreasing amounts as the crack advanced under sustained load. An example of a cleaved region embedded in a matrix of microvoid coalescence in this specimen is shown in Fig. 11.

Ratios of applied stress to yield stress are encircled in figures containing PTC specimen data; these imply directly the reductions in load-carrying capacity owing to SLC. For example, in the case of alloy R23A, the fracture resistance inferred from the rising-load tests suggests that the fracture-safe, load-carrying limit is approximately 90% of the yield limit load, while fracture resistance implied from the threshold K_{It} indicates a fracture-safe, load-carrying limit which is only 70% of the yield limit load.

DISCUSSION

While variations in Δ from plate to plate, for a given crack orientation, do not seem to correlate with differences in hydrogen content (among other parameters), it must be cautioned that invalidity of the fracture toughness numbers (cf. Eqs. (4) and (5)) makes quantitative comparisons between materials uncertain. The results of Sandoz (5), for example, suggest that the apparent degradation for a given material and crack orientation depends on specimen thickness, i.e., the degree of constraint relaxation. Thus it would be most appropriate to normalize all of the present results to the same level of constraint

Table 1
Properties of Ti-6Al-4V Alloys

NRL Alloy	Specimen Type		Hydrogen ppm	Oxygen ppm	σ_{ys} ksi (MPa)	Rolling Temp. °F (°K)	Forge Temp. Range	K_{Ir}		K_{Ic} Criteria		K_{It} ksi $\sqrt{in.}$ (MPa – $m^{1/2}$)	$2.5(K_{It}/\sigma_{ys})^2 \leqslant B$	SLC Degradation Δ(%)
	SEN Bend	PTC Tension						K_Q ksi $\sqrt{in.}$ (MPa – $m^{1/2}$)	K_{Imax} ksi $\sqrt{in.}$ (MPa – $m^{1/2}$)	$P_{max}/P_Q \leqslant 1.10$	$2.5(K_Q/\sigma_{ys})^2 \leqslant B$, a, D–a			
D4	X		40	500	115 (803)	1700 (1200)	β	68 (76)	80 (89)	no	no	70 (78)	no	13
C5	X		70	1100	133 (928)	1700 (1200)	α+β	56 (62)	58 (65)	yes	yes	46 (51)	yes	21
		X							95 (106)			66 (73)	yes	31
D3	X		56	1500	119 (831)	1900 (1311)	β	73 (81)	80 (89)	yes	no	65 (72)	yes	19
R23A	X		35	1600	144 (1005)			66 (73)	82 (91)	no	no	53 (59)	yes	35
		X							121 (135)			86 (96)	no	29
D2	X		80	1500	143 (998)	1400 (1033)	β	48 (53)	49 (55)	yes	yes	43 (48)	yes	12
D1	X		47	1500	131 (914)	1700 (1200)	β	46 (51)	47 (52)	yes	yes	42 (47)	yes	11
D5	X		57	1500	133 (928)	1700 (1200)	α+β	41 (46)	42 (47)	yes	yes	37 (41)	yes	12
		X							71 (79)			48 (53)	yes	32
R14A		X	50	600	125 (873)				120 (133)			102 (113)	no	15

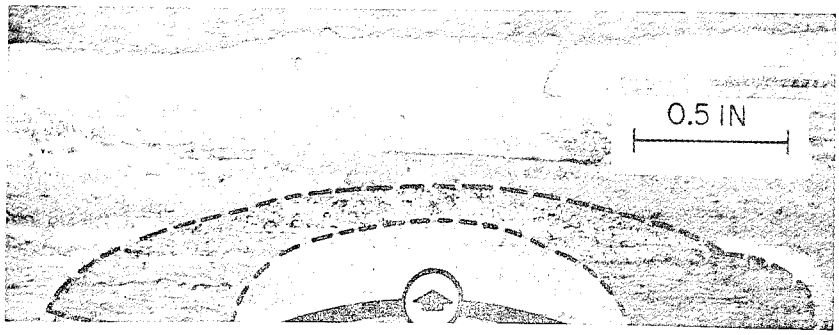

Fig. 10—Anisotropic crack growth in a PTC tension specimen of NRL alloy R23A under sustained load: SLC growth (bounded by dashed line) is less in thickness direction (denoted by arrow) than in transverse direction.

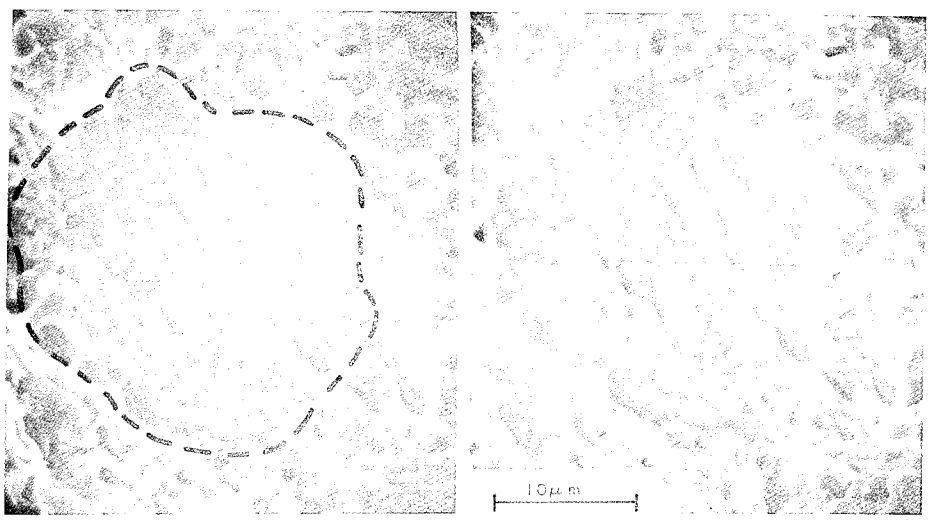

Fig. 11—Stereoscopic pair of scanning electron micrographs illustrate cleaved region (within dashed loop) embedded in matrix of coalesced microvoids, from SEN bend specimen of NRL alloy R23A, cracked under sustained load with K_{Ii} = 65 ksi$\sqrt{\text{in.}}$ (74 MPa-m$^{1/2}$)

(or relaxation thereof); unfortunately, fracture mechanics has yet to be developed to this capability.

However, most of the threshold K_{It} values do meet the ASTM thickness requirement

$$2.5 \left(\frac{K_{It}}{\sigma_{ys}}\right)^2 \leq B \tag{6}$$

for validity, and thus may be useful for fracture mechanics interpretations of flaw size vs stress level relationships. Hence the SLC effect may be reckoned with in much the same

manner that stress-corrosion-cracking effects are factored into fracture-safe design procedures, as described by Judy and Goode (1) and Pellini (16). For plates of those materials which do not satisfy Eq. (6), viz. alloys D4, R14A, and R23A (PTC specimen, TS orientation), flaw size vs stress level relationships independent of thickness cannot be inferred.

Perhaps it is worth emphasizing that a fracture toughness number K_{It} in Table 1 which satisfies Eq. (6) appears to represent a more conservative fracture-safe design parameter than a K_{Ic} number, determined from a rising-load test, in accordance with ASTM specifications, which cannot account for insidious time-delayed failures owing to SLC. For example, in the case of alloy C5 (SEN specimen data) the K_Q value of 56 ksi$\sqrt{\text{in.}}$ (62.3 MPa-m$^{1/2}$), which is a close approximation to K_{Ic}*, implies a fracture resistance some 21% higher than the threshold K_{It} = 46 ksi$\sqrt{\text{in.}}$ (51.2 MPa-m$^{1/2}$) determined from sustained-load, cantilever bend tests.

To investigate any potential role which hydrogen may have in SLC, an analysis of crack growth rate data might prove useful in detecting an incubation time τ (7, 17, 18) associated with this cracking. Such a τ should exist if a critical concentration of hydrogen c must accumulate at the crack tip before cracking can proceed. Hydrogen might so accumulate by diffusing from the bulk by interaction with the crack-tip stress field as modeled by Liu (19), with the result that

$$c = c_0 \exp\left(\frac{AK_{Ii}}{kT\sqrt{r}} \cos\frac{\theta}{2}\right) , \tag{7}$$

where

c_0 = concentration of hydrogen in the bulk

A = lumped material constant

k = Boltzmann's constant

T = absolute temperature

r, θ = polar coordinates emanating from crack tip.

By using the compliance technique (2), crack growth rate data shown in Fig. 12 have been obtained from the SEN specimen of alloy D3, which was loaded initially to K_{Ii} = 66.6 ksi$\sqrt{\text{in.}}$ (74.1 MPa-m$^{1/2}$) and failed under sustained load in room air after about 1.5 hr. Clearly the data in Fig. 12 do not reveal an incubation period, as crack growth begins almost immediately, at rates of the order of 10^{-5} in./s (10^{-5} cm/s). If the high mobility of interstitial hydrogen has made the incubation period undetectably small at room temperature, then lower temperatures can be used to increase the extent of any incubation period, which should vary inversely with drift velocity of the hydrogen. The drift velocity used by Cottrell and Bilby (20, 21) in relating solute interaction with a dislocation stress field is given by Einstein's theory of Brownian motion as

*Supplementary tests with non-sidegrooved specimens, with D = 2.0 in. (5.08 cm), indicated that K_{Ic} = 55.4 ksi$\sqrt{\text{in.}}$ (61.6 MPa-m$^{1/2}$), as determined in strict accord with ASTM procedures. Similarly, for alloy D3, K_{Ic} = 71.8 ksi$\sqrt{\text{in.}}$ (79.9 MPa-m$^{1/2}$), which compares well with the value K_Q reported in Table 1, 73 ksi$\sqrt{\text{in.}}$ (81.2 MPa-m$^{1/2}$).

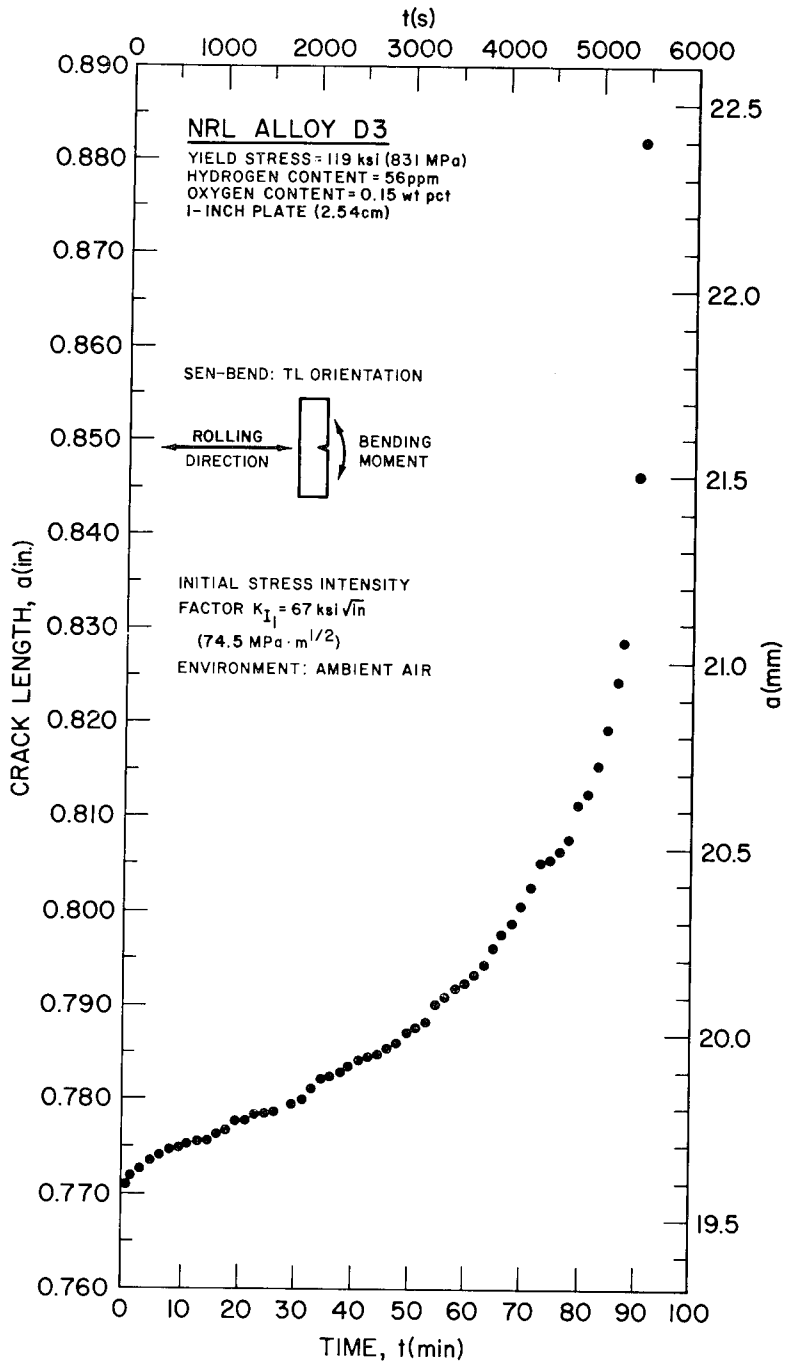

Fig. 12—Crack extension in a SEN bend specimen of NRL alloy D3 under sustained load with K_{Ii} = 67 ksi$\sqrt{in.}$ (74 MPa-m$^{1/2}$)

$$\bar{v} = -\left(\frac{D}{kT}\right) \nabla V, \tag{8}$$

where D is the diffusivity and V the interaction energy. Liu (19) expresses the interaction energy between the diffusing hydrogen and the stress field of the crack tip as

$$V = -\frac{AK_{Ii}}{\sqrt{r}} \cos\frac{\theta}{2} \quad . \tag{9}$$

From Eqs. (8) and (9) it follows that the incubation time is given by

$$\tau = \frac{2LkTr^{3/2}}{AK_{Ii}\, D_0 \exp\left(\frac{-Q}{kT}\right)} \quad , \tag{10}$$

where

L = a constant with the dimension of length

D_0 = the diffusion constant

Q = the activation energy.

At this point, however, any participation of hydrogen in the SLC process remains undefined.

Furthermore, a recent study by Meyn (22) showed that for one Ti-6A1-4V alloy the SLC effect failed to disappear at an exceedingly low hydrogen level (i.e., a few ppm) which bordered on the limit of detection. Thus it is not clear that SLC in titanium alloys is caused solely by internal hydrogen content. In other studies of SLC in inert environments, it has been noted that crack growth occurs with an initial region of transient growth, followed by a region of steady state growth, and terminating with a region of accelerating growth which leads to failure; this appears to be the pattern in Fig. 12. Such behavior has in some instances been relatable to material flow properties (23). Similar efforts might prove fruitful in the present case to interpret room-temperature crack growth rate data.

SUMMARY

Degradation in load-carrying capability owing to SLC is widespread and serious in alloys of the Ti-6A1-4V family. Each of eight plate samples tested in air at room temperature exhibited the effect, with degradations ranging from 11 to 35%. The amount of degradation does not seem to correlate with interstitial contents, processing variables, or strength and toughness levels; however, the susceptibility to SLC is orientation dependent. For most of the materials examined, invalidity of the rising-load fracture toughness values with respect to plane-strain criteria makes quantitative comparison of degradations uncertain.

If the potential hazard of time-delayed catastrophic failures owing to SLC is to be avoided in structures fabricated with these alloys, the SLC effect is one that must be reckoned with, in much the same manner that stress-corrosion-cracking effects are factored into fracture-safe design procedures. It appears for most materials examined that the threshold stress-intensity factor K_{It}, below which time-delayed failures owing to SLC do not occur, may be useful for fracture mechanics interpretations of flaw size vs stress level relationships. While there is no standard technique for determining such a threshold,

it appears that K_{It} represents a more conservative, fracture-safe design parameter than K_{Ic}, determined from a rising load test in conformity with ASTM specifications, which cannot account for insidious time-delayed failures owing to SLC.

The mechanism of SLC has yet to be defined, especially with regard to the possible role of interstitial hydrogen.

ACKNOWLEDGMENTS

The authors gratefully acknowledge Messrs. S. J. McKaye, R. J. Hicks, and M. L. Cigledy for very able assistance with the experimental phase of this work, and the Office of Naval Research for financial support.

REFERENCES

1. R. W. Judy Jr., and R. J. Goode, "Stress-Corrosion-Cracking Characterization Procedures and Interpretations to Failure-Safe Use of Titanium Alloys," Trans. ASME, J. Basic Eng. **91** (Series D, No. 4), 614 (Dec. 1969).
2. H. R. Smith and D. E. Piper, "Stress Corrosion Testing With Precracked Specimens," Ch. 2 in *Stress-Corrosion Cracking in High Strength Steels and in Titanium and Aluminum Alloys* (B. F. Brown, ed.), Naval Research Laboratory, Washington, D.C., 1972, pp. 17-77.
3. B. F. Brown, "The Application of Fracture Mechanics to Stress-Corrosion Cracking," Met. Rev. 129, Met. Mater. **2**, 171 (1968).
4. H. M. Burte, E. F. Erbin, G. T. Hahn, R. J. Kotfila, J. W. Seeger, and D. A. Wruck, "Hydrogen Embrittlement of Titanium Alloys," Met. Prog. **67**, 115 (May 1955).
5. G. Sandoz, "Subcritical Crack Propagation in Ti-8A1-1Mo-1V Alloy in Organic Environments, Salt Water and Inert Environments," in *Proceedings of Conference on Fundamental Aspects of Stress Corrosion Cracking* (R. W. Staehle et al., ed.), NACE, Houston, Texas, 1969, pp. 684-690.
6. D. A. Meyn, "Effect of Hydrogen Content on Hydrogen-Induced Cracking of Ti-8A1-1Mo-1V," *Report of NRL Progress*, Dec. 1971, pp. 11-12.
7. A. R. Troiano, "The Role of Hydrogen and Other Interstitials in the Mechanical Behavior of Metals," 1959 Campbell Memorial Lecture, ASM Trans. **52**, 54 (1960).
8. H. P. Chu, "Fracture Characteristics of Titanium Alloys in Air and Seawater Environment," Eng. Fr. Mech. **4**, 107 (1972).
9. I. R. Lane, Jr., J. L. Cavallaro, and A. G. S. Morton, "Sea-Water Embrittlement of Titanium," in *Stress Corrosion Cracking of Titanium*, ASTM STP 397, Amer. Soc. Testing Mater., Philadelphia, Pa., 1966, p. 246.
10. "Progress in Measuring Fracture Toughness and Using Fracture Mechanics, Fifth Report of a Special ASTM Committee," J. R. Low, Jr., Chmn., Mater. Res. Stand. **4**, 107 (Mar. 1964).
11. B. F. Brown, "A New Stress-Corrosion Cracking Test for High-Strength Alloys," Mater. Res. Stand. **6**, 129 (1966).

12. F. R. Stonesifer, "Fracture Toughness Equations for Bend Specimens," *Report of NRL Progress*, Feb. 1968, pp. 12-13.

13. C. F. Tiffany and J. N. Masters, "Applied Fracture Mechanics," in *Fracture Toughness Testing and Its Applications*, ASTM STP 381, Amer. Soc. Testing Mater., Philadelphia, Pa., 1965, p. 249.

14. R. J. Goode, "Identification of Fracture Plane Orientation," Mater. Res. Stand. **12**, 31 (Sep. 1972).

15. E 399-72, "Standard Method of Test for Plane-Strain Fracture Toughness of Metallic Materials," 1972 Annual Book of ASTM Standards, Part 31, Amer. Soc. Testing Mater., Philadelphia, Pa., 1972, pp. 955-974.

16. W. S. Pellini, "Integration of Analytical Procedures for Fracture-Safe Design of Metal Structures," NRL Report 7251, Mar. 26, 1971.

17. C. S. Kortovich and E. A. Steigerwald, "A Comparison of Hydrogen Embrittlement and Stress Corrosion Cracking in High-Strength Steels," Eng. Fr. Mech. 4, 637 (Dec. 1972).

18. R. P. Wei, S. R. Novak, and D. P. Williams, "Some Important Considerations in the Development of Stress Corrosion Cracking Test Methods," Mater. Res. Stand. **12**, 25 (Sep. 1972).

19. H. W. Liu, "Stress-Corrosion Cracking and the Interaction Between Crack-Tip Stress Field and Solute Atoms," Trans. ASME, J. Basic Eng. 92, 633 (Sep. 1970).

20. A. H. Cottrell, "Effect of Solute Atoms on the Behaviour of Dislocations," *Report of a Conference on Strength of Solids*, The Physical Society, London, England, 1948, pp. 30-38.

21. A. H. Cottrell and B. A. Bilby, "Dislocation Theory of Yielding and Strain Ageing of Iron," Proc. Phys. Soc. London Sect. A, **62**, 49 (1949).

22. D. A. Meyn, "A Procedure for Investigating the Effect of Hydrogen Content on Toughness and Sustained Load Cracking Resistance of Titanium Alloys, With Some Results for Ti-6A1-4V," NRL Memorandum Report 2461 (June 1972).

23. J. D. Landes and R. P. Wei, "Kinetics of Subcritical Crack Growth and Deformation in a High Strength Steel," Trans. ASME, J. Eng. Mater. Tech. 95 (Series H, No. 1), 2 (Jan. 1973).